COMPREHENSIVE STUDIES OF PIEZO-OPTICAL EFFECT IN LANGASITE CRYSTALS

B.H. MYTSYK, A.S. ANDRUSHCHAK[1], G.I. GASKEVICH

Karpenko Physicomechanical Institute, Nat. Acad. Sci. of Ukraine
(5, Naukova Str., Lviv 79601, Ukraine; e-mail: mytsyk@ipm.lviv.ua),

[1]**Lviv Polytechnic National University**
(12, St. Bandera Str., Lviv 79013, Ukraine)

UDC 535.551:548.0

The specific features of the procedure of determination of the absolute piezo-optical coefficients (POCs) for real specimens which are characterized, as a rule, by a slight out-of-parallelism of their faces of about $(2 \div 4) \times 10^{-2}$ deg are described. The technique has been applied to study langasite $La_3Ga_5SiO_{11}$ crystals. Besides the absolute POCs, which couple the changes of refractive indices with the mechanical stresses, the birefringence and path-difference POCs are also determined. The correlation between the indicated POCs, which confirmed the unambiguity and reliability of the results obtained, has been studied in detail. The comparative researches of piezo-optical effects in langasite crystals and reference crystals of lithium niobate have been carried out as well. Since the values of some POCs for both crystals turned out comparable, a conclusion has been drawn that langasite is a promising substance for the application in acousto-optical devices since langasite crystals are characterized by a high thermal stability of their physical parameters.

1. Introduction

Crystals of lanthanum gallium silicate (langasite) $La_3Ga_5SiO_{11}$ were grown for the first time a quarter of a century ago; they turned out a unique piezoelectric material [1, 2]. By their piezoelectric and electromechanical parameters, they are not inferior to lithium niobate crystals [3], and, by the thermal stability of those characteristics, they are several times superior to the latter. Therefore, langasite crystals find a wide use in applied branches. The optical characteristics of langasite have been studied as well [4]; however, the dependence of its optical properties on external fields (photoelastic and acousto-optical effects) has not been analyzed. The lack of those data does not allow one to estimate the potentiality of applications of $La_3Ga_5SiO_{11}$ crystals in the problems of applied optics.

As for the electro-optical effect in langasite crystals, it has been studied adequately [5]. By the values of electro-optical coefficients, langasite is 4–8 times inferior to reference potassium dihydrogen phosphate (KDP) crystals [6] and more than an order of magnitude to lithium niobate ones [7, 8]. Therefore, it cannot compete with the latter on the market of electro-optical applications.

In this work, we studied the piezo-optical effect (POE) in langasite crystals, namely, the absolute piezo-optical coefficients (POCs) π_{im}, as well as the POCs of birefringence, π^*_{km}, and path difference, π^0_{km}. The subscripts i, k, and m designate the directions of the electric vector of the light wave, light propagation, and uniaxial pressure, respectively, in the crystal-optical coordinate system.

Knowing the entire POC matrix π_{im}, one can calculate all elasto-optical coefficients p_{in} (n is the deformation direction), construct the indicating surfaces of the elasto-optical effect and the effects of acousto-optical quality, and, making use of those surfaces, estimate the langasite application efficiency in acousto-optical devices. We emphasize that the determination of the p_{im} coefficient matrix on the basis of the POC matrix and the tensor relation $p_{in} = \pi_{im}C_{mn}$, where C_{mn} are the elastic stiffness constants, is the only method that allows the values of the quantities p_{in}, including their signs, to be determined correctly and unequivocally. The POCs of path difference π^0_{km} and birefringence π^*_{km} were

determined in this work in order to verify the reliability of the procedure of finding the absolute coefficients π_{im}.

2. Modified Technique for the Determination of the POCs π_{im}

The coefficients π_{im} were determined making use of the Mach–Zender interferometric method. Specimens $8\times8\times8$ mm^3 in dimensions were studied. The optical path length for a light beam in the interferometer's shoulder, where the specimen is mounted, can be written down as $\Delta_k = n_i d_k$, where n_i is the refractive index of the crystal, and d_k is the specimen's thickness measured along the direction of beam propagation. Then, if the specimen is undergone the action of the mechanical stress σ_m, the variation of the optical path length is given by the expression [9]

$$\delta\Delta_k = \delta n_i d_k + \delta d_k (n_i - 1), \tag{1}$$

where the factor $(n_i - 1)$ takes into consideration that the specimen, being deformed by the magnitude δd_k, reduces the optical path by the value of $n_c \delta d_k = \delta d_k$, where $n_c = 1$ is the refractive index of air.

Taking advantage of the Hooke law $\delta d_k/d_k = S_{km}\sigma_m$, where S_{km} are the elastic compliance constants, and the well-known formula of piezo-optics [9, 10]

$$\delta n_i = -\frac{1}{2}\pi_{im}\sigma_m n_i^3, \tag{2}$$

we obtain

$$\delta\Delta_k = -\frac{1}{2}\pi_{im}\sigma_m n_i^3 d_k + S_{km}\sigma_m d_k (n_i - 1). \tag{3}$$

Expressions (1) and (3) are valid for a specimen with perfectly parallel faces. The faces of real crystalline specimens are always characterized by a certain out-of-parallelism of the wedge type: $a/l = \tan\alpha \approx \alpha$. If the variation a of specimen's thickness owing to the out-of-parallelism of its faces is about $5 \div 10$ μm within the specimen's length $l \approx 8$ mm measured along the direction of the force F_m (see Fig. 1), then $\alpha = (2 \div 4) \times 10^{-2}$ deg. Under the action of the mechanical stress $\sigma_m = 100$ kG/cm, the center of the specimen becomes shifted by $\delta l = 4\times10^{-2}$ mm, and the specimen's thickness varies by $\delta^* d_k = a\delta l/l = 50$ nm at the point of light beam incidence (Fig. 1). The corresponding change of the optical path length is equal to $\delta^*\Delta_k = n_i\delta^* d_k$; so that, for langasite ($n_i \approx 2$ [4, 5]), the variation is about 100 nm.

If the POCs π_{im} are determined by the method of half-wave stresses σ_{im} (in this case, $\delta\Delta_k = \lambda/2$, where

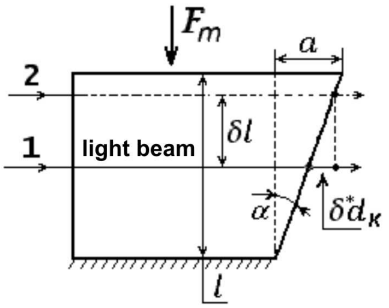

Fig. 1. Scheme of the error $\delta^* d_k$ emergence: (*1*) a beam at $F_m = 0$, (*2*) a beam at $F_m \neq 0$

λ is the light wavelength), the determination error for σ_{im} and, correspondingly, π_{im} – owing to the existence of the determination error for $\delta^*\Delta_k$ – is equal to $\beta_{\text{wedge}} = \delta^*\Delta_k/\delta\Delta_k = 2\delta^*\Delta_k/\lambda \approx 32\%$. It is clear that the higher is the half-wave stress σ_{im}, the larger are the values of $\delta^* d_k$, $\delta^*\Delta_k$, and β_{wedge}.

2.1. Elimination of the face tapering-induced error $\delta^*\Delta_k$

In order to eliminate the face tapering-induced error, we must determine the half-wave stress two times: after the value of σ_{im} having been measured once, the specimen should be rotated by 180° along the direction of the force F_m, that is around the direction of propagation of light beam *1* (Fig. 1), and a new value of the half-wave stress – we designate it as σ'_{im} – should be measured. The error $\delta^*\Delta_k$ is included into the corresponding relations for σ_{im} and σ'_{im} with opposite signs.

For the half-wave method of researches (in this case, $\delta\Delta_k = \lambda/2$ and $\sigma_m = \sigma_{im}$) and taking the error $\delta^*\Delta_k$ into account, Eq. (3) reads

$$\delta\Delta_k = \lambda/2 = -\frac{1}{2}\pi_{im}\sigma_{im} n_i^3 d_k +$$

$$+ S_{km}\sigma_{im} d_k (n_i - 1) + \delta^*\Delta_k. \tag{4}$$

Equation (4) includes the half-wave stress σ_{im}. The same quantity should be substituted into the analogous equation for the specimen rotated by 180 °C along the direction m. As a result, we obtain

$$\delta\Delta'_k = -\frac{1}{2}\pi_{im}\sigma_{im} n_i^3 d_k + S_{km}\sigma_{im} d_k (n_i - 1) - \delta^*\Delta_k. \tag{5}$$

Since the mechanical stresses σ_{im} in Eqs. (4) and (5) are identical, identical are also the absolute values of the

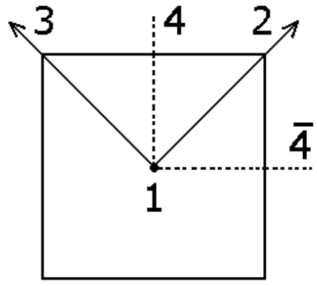

Fig. 2. Specimen orientation for the determination of POCs π_{14}, π_{41}, and π_{44}

error $\delta^*\Delta_k$. Therefore, having added Eqs. (4) and (5), we get rid of this quantity:

$$\delta\Delta_k + \delta\Delta'_k = -\pi_{im}\sigma_{im}n_i^3 d_k + 2S_{km}\sigma_{im}d_k(n_i - 1). \quad (6)$$

If Eq. (5) have included the half-wave stress σ'_{im}, the relation $\delta\Delta'_k = \lambda/2$ would have been true. The stress σ_{im}, however, is active; therefore, the value of $\delta\Delta'_k$ differs from that of $\lambda/2$, and

$$\delta\Delta'_k = \frac{\lambda}{2}\frac{\sigma_{im}}{\sigma'_{im}}. \quad (7)$$

Substituting Eq. (7) into Eq. (6) and taking into account that $\delta\Delta_k = \lambda/2$, we obtain the ultimate relation for the determination of the POCs π_{im} on the basis of experimental values of the quantities σ_{im} and σ'_{im}:

$$\pi_{im} = -\frac{\lambda}{2n_i^3 d_k}\left(\frac{1}{\sigma_{im}} + \frac{1}{\sigma'_{im}}\right) + \frac{2S_{km}}{n_i^3}(n_i - 1). \quad (8)$$

If there is no specimen tapering, then $\sigma_{im} = \sigma'_{im}$. Provided that this condition is satisfied, Eq. (8) transforms into the known relation for a specimen with parallel faces.

3. Features of Calculation Procedure for Absolute POCs π_{im}

1. The calculations of POCs π_{im} were carried out on the basis of Eq. (8) and making use of the experimental values for driving mechanical stresses $\sigma^0_{im} = d_k\sigma_{im}$ and $\sigma'^0_{im} = d_k\sigma'_{im}$, which characterize the induced variation of the optical path length. One should bear in mind that the driving stress, which has the physical meaning of the half-wave stress in a specimen with unit dimensions (a cube with a 1-cm edge length), is a characteristic of the material, whereas the half-wave stress is a characteristic of the specimen. The signs (plus or minus) of σ^0_{im} and σ'^0_{im} mean whether the variation $\delta\Delta_k$ induced by the applied mechanical stress increases or diminishes, respectively, the absolute value of the optical path length for the light beam that passes through the specimen. The required signs could be determined with the help of a plane-parallel plate located on the path of the beam transversing the specimen, and the corresponding values should be inserted into expression (8) before λ. If the plate should deviate from the orientation perpendicular to the beam, its effective thickness and the optical path length of the beam would become larger. In this case, the interference bands would become shifted towards a definite side. If the action of the stress σ_{im} gives rise to the displacement of those bands in the same direction, the signs of $\delta\Delta_k$ and σ_{im} are positive, and *vice versa.* In addition, the calculation procedure should take into account that the minus sign is associated with the mechanical stresses of compression.

Note that relation (8) is satisfied only for the principal POCs π_{im} with m and $i = 1$, 2, and 3. For nonprincipal POCs π_{14}, π_{41}, and π_{44}, the relevant relations of type (8) become more complicated at the expense of the complicated expressions that involve those POCs. The relevant expressions, as well as the corresponding experimental conditions for a specimen with X-45°-orientation (Fig. 2), are as follows:
for the POC π_{14} and experimental conditions $i = 1$, $k = \bar{4}(4)$, and $m = 4(\bar{4})$,

$$\delta\Delta_{\bar{4}(4)} = -\frac{\pi_{12} + \pi_{13} \pm \pi_{14}}{4}\sigma n_1^3 d_{\bar{4}(4)} +$$

$$+\frac{1}{4}(S_{11} + S_{33} - S_{44} + 2S_{13})\sigma d_{\bar{4}(4)}(n_1 - 1); \quad (9)$$

for π_{41} and conditions $i = 4(\bar{4})$, $k = \bar{4}(4)$, and $m = 1$,

$$\delta\Delta_{\bar{4}(4)} = -\frac{\pi_{21} + \pi_{31} \pm 2\pi_{41}}{4}\sigma n_4^3 d_{\bar{4}(4)} +$$

$$+\frac{1}{2}(S_{12} + S_{13} \mp S_{14})\sigma d_{\bar{4}(4)}(n_4^3 - 1); \quad (10)$$

and for π_{44} and conditions $i = 4(\bar{4})$, $k = \bar{4}(4)$, and $m = 4(\bar{4})$,

$$\delta\Delta_{\bar{4}(4)} = -\frac{\pi_{11} + \pi_{13} \mp \pi_{14} + \pi_{31} + \pi_{33} \mp 2\pi_{41} + 2\pi_{44}}{8}\times$$

$$\times\sigma n_4^3 d_{\bar{4}(4)} + \frac{1}{4}(S_{11} + S_{33} - S_{44} + 2S_{13})\sigma d_{\bar{4}(4)}(n_4^3 - 1). \quad (11)$$

In expressions (9)–(11), the lower signs correspond to symmetric experimental conditions, and the corresponding values of i, k, and m are indicated in parentheses.

2. Now, let us derive a relation for the determination of the POC π_{14}. For this purpose, we use Eq. (9) that corresponds to the direct and symmetric experimental conditions. First, we rewrite expression (9) in form (4) modified for conditions $i = 1$, $k = \bar{4}$, and $m = 4$:

$$\delta\Delta_{\bar{4}} = \lambda/2 = -\frac{1}{2}\pi^{\Sigma}_{14}\sigma_{14}n_1^3 d_{\bar{4}} +$$

$$+S^{\Sigma}_{\bar{4}4}\sigma_{14}\cdot d_{\bar{4}}(\mathrm{n}_1 - 1) + \delta\Delta^{*}_{\bar{4}}, \qquad (12)$$

where

$$\pi^{\Sigma}_{14} = \frac{1}{2}(\pi_{12} + \pi_{13} + \pi_{14}),$$

$$S^{\Sigma}_{\bar{4}4} = \frac{1}{4}(S_{11} + S_{33} - S_{44} + 2S_{13}). \qquad (13)$$

Writing down a similar equation for the specimen, which is rotated by 180° along the direction of the force F_m, we obtain, by analogy with Eqs. (4)–(8),

$$\pi^{\Sigma}_{14} = -\frac{\lambda}{2n_1^3 d_{\bar{4}}}\left(\frac{1}{\sigma_{14}} + \frac{1}{\sigma'_{14}}\right) + \frac{2S^{\Sigma}_{\bar{4}4}}{n_1^3}(n_1 - 1). \qquad (14)$$

For symmetric experimental conditions $i = 1$, $k = 4$, and $m = \bar{4}$, we have

$$\pi^{\Sigma}_{1\bar{4}} = -\frac{\lambda}{2n_1^3 d_4}\left(\frac{1}{\sigma_{1\bar{4}}} + \frac{1}{\sigma'_{1\bar{4}}}\right) + \frac{2S^{\Sigma}_{\bar{4}4}}{n_1^3}(n_1 - 1), \qquad (15)$$

where

$$\pi^{\Sigma}_{1\bar{4}} = \frac{1}{2}(\pi_{12} + \pi_{13} - \pi_{14}), \quad S^{\Sigma}_{\bar{4}4} = S^{\Sigma}_{4\bar{4}}. \qquad (16)$$

Subtracting Eq. (15) from Eq. (14), we get rid of the "elastic" term, as well as of the principal POCs π_{12} and π_{13}, which allows us to calculate the quantity π_{14} more exactly. As a result, we obtain

$$\pi_{14} = -\frac{\lambda}{2n_1^3}\left(\frac{1}{\sigma_{14}d_{\bar{4}}} + \frac{1}{\sigma'_{14}d_{\bar{4}}} - \frac{1}{\sigma_{1\bar{4}}d_4} - \frac{1}{\sigma'_{1\bar{4}}d_4}\right) =$$

$$= -\frac{\lambda}{2n_1^3}\left(\frac{1}{\sigma^0_{14}} + \frac{1}{\sigma'^0_{14}} - \frac{1}{\sigma^0_{1\bar{4}}} - \frac{1}{\sigma'^0_{1\bar{4}}}\right). \qquad (17)$$

Analogous reasons applied to Eq. (10) bring about the relation for the determination of POC π_{41}:

$$\pi_{41} = -\frac{\lambda}{4n_4^3}\left(\frac{1}{\sigma^0_{41}} + \frac{1}{{\sigma'_{41}}^0} - \frac{1}{\sigma^0_{\bar{4}1}} - \frac{1}{{\sigma'_{\bar{4}1}}^0}\right) - S_{14}\frac{n_4 - 1}{n_4^3}, \qquad (18)$$

where $n_4 = \sqrt{2}n_1n_3/\sqrt{n_1^2 + n_3^2}$ is the index of refraction in the crystal along the direction $i = 4$ or $i = \bar{4}$ (see Fig. 2).

3. Adding and subtracting the expressions for the POCs π^{Σ}_{44} and $\pi^{\Sigma}_{\bar{4}4}$, which are similar to Eqs. (14) and (15), respectively, and modifying them to the case of direct and symmetric conditions for Eq. (11), we obtain another relation for the calculation of π_{41} (for absolutely different experimental conditions), as well as a cumbersome but only possible relation for the determination of the POC π_{44} on the basis of driving stresses σ^0_{im}, the coefficients S_{km}, and the preliminarily determined values of other POCs:

$$\pi_{41} + \frac{1}{2}\pi_{14} = \frac{\lambda}{2n_4^3}\left(\frac{1}{\sigma^0_{44}} + \frac{1}{{\sigma'_{44}}^0} - \frac{1}{\sigma^0_{\bar{4}4}} - \frac{1}{{\sigma'_{\bar{4}4}}^0}\right), \qquad (19)$$

$$\pi_{44} + \frac{1}{2}(\pi_{11} + \pi_{13} + \pi_{31} + \pi_{33}) = -\frac{\lambda}{2n_4^3}\Big(\frac{1}{\sigma^0_{44}} + \frac{1}{\sigma'^0_{44}} +$$

$$+\frac{1}{\sigma^0_{\bar{4}4}} + \frac{1}{\sigma'^0_{\bar{4}4}}\Big) + (S_{11} + S_{33} - S_{44} + 2S_{13})\frac{n_4 - 1}{n_4^3}. \qquad (20)$$

4. The calculations of the coefficient π_{41} by expressions (18) and (19) bring about different results. But if the coefficient $S_{14} = -3.6$ Br [2] (1 Br (Brewster) $= 10^{-12}$ m^2/N) reverses its sign, those results become comparable. We managed to resolve the problem of the amplitude and the sign of S_{14} in the following way. If, under the direct and symmetric conditions of Eq. (10), the light polarization is changed from $i = 4(\bar{4})$ to $i = 1$ (by rotating the polarizer by 90°), the "piezo-optical" term in Eq. (10) will contain only the coefficient π_{11}, while the "elastic" term will not be changed, because the direction of light propagation will remain the same. This means that Eq. (10) for $i = 1$ looks like

$$\delta\Delta_{4(\bar{4})} = -\frac{1}{2}\pi_{11}\sigma n_1^3 d_{4(\bar{4})} +$$

$$+\frac{1}{2}(S_{12} + S_{13} \mp S_{14})\sigma d_{4(\bar{4})}(n_4 - 1). \qquad (21)$$

Now, writing down, by analogy with formula (14), the expression for $\pi^{\Sigma}_{11} = \pi_{11}$ at $k = \bar{4}$,

$$\pi^{\Sigma}_{11} = \pi_{11} = -\frac{\lambda}{2n_1^3 d_{\bar{4}}}\left(\frac{1}{\sigma_{11(k=\bar{4})}} + \frac{1}{\sigma'_{11(k=\bar{4})}}\right) +$$

$$+(S_{12}+S_{13}-S_{14})\frac{n_1-1}{n_1^3}, \qquad (22)$$

and a similar expression for $\pi_{11}^{\Sigma}=\pi_{11}$ at $k=4$ (in the latter case, the sign of S_{14} in the "elastic" term is changed), and subtracting the expressions obtained, we arrive at a formula for the calculation of S_{14} on the basis of either the half-wave stresses σ_{11} and σ'_{11} or the driving stresses $\sigma_{11}^0=d_{\bar{4}(4)}\sigma_{11}$ and $\sigma_{11}'^0=d_{\bar{4}(4)}\sigma'_{11}$ in two geometries ($k=\bar{4}$ and $k=4$):

$$S_{14}=\frac{\lambda}{4(n_1-1)}\left[\left(\frac{1}{\sigma_{11}^0}+\frac{1}{\sigma_{11}'^0}\right)_{k=\bar{4}}-\right.$$

$$\left.-\left(\frac{1}{\sigma_{11}^0}+\frac{1}{\sigma_{11}'^0}\right)_{k=4}\right]. \qquad (23)$$

Substituting the values of σ_{11}^0 and $\sigma_{11}'^0$ for $k=\bar{4}$ (rows 17 and 18 in Table 1) and $k=4$ (rows 19 and 20 in Table 1) into Eq. (23), we obtain $S_{14}=+(3.65\pm0.4)$ Br. The absolute value of S_{14} accurately corresponds, within the indicated experimental error, to the results of work [2]; however, the sign is different. For this value of S_{14} and the values of σ_{41}^0 and $\sigma_{\bar{4}1}^0$ from Table 1, Eq. (18) yields $\pi_{41}=+(0.36\pm0.14)$ Br, while Eq. (19) gives rise to $\pi_{41}=+(0.3\pm0.1)$ Br. The arithmetic-mean error between those values amounts to 9%, being smaller than the determination error of the POC π_{41} itself. A more detailed discussion concerning the determination errors of the absolute values of the POCs is presented in Section 4. Notice also that relation (22) for $k=\bar{4}$ and an analogous relation for $k=4$ allow the POC π_{11} to be determined in two more independent experimental geometries (rows 17 and 19 in Table 1) for a specimen with 45°-orientation with respect to the optical indicatrix axes X_2 and X_3 (Fig.2).

For specific evaluations of S_{14}, the POC π_{41}, and other POCs π_{im} (see Table 1), we used the values of refractive indices for langasite crystals taken from works [4, 5]: $n_1=n_2=n_o=1.8993$ and $n_3=n_e=1.9107$; the birefringence is , accordingly, $\Delta n=0.0114$; all the parameters are quoted for $\lambda=0.633$ μm. The values of elastic compliances S_{km} – $S_{11}=+8.76$ Br, $S_{33}=+5.59$, $S_{12}=-4.03$, $S_{13}=-1.85$, and $S_{44}=+21.0$ – were taken from work [2].

5. We recall that, while determining the nonprincipal POCs π_{14}, π_{41}, and π_{44}, it is important to fix either the positive directions of the axes X_2 and X_3 or the directions 4 and $\bar{4}$ (see Fig. 2). This can be done on the basis of the piezoelectric effect in crystals, which belong to polar classes of symmetry, or on the basis of the piezo-optical effect in arbitrary crystals, by fixing the positive sign of that POC, which is the simplest for determination, e.g., π_{14}. A more detailed discussion on this topic can be found in work [11] or in review [9]. In this work, the directions 4 and $\bar{4}$ are fixed on the basis of the criterion $\pi_{14}>0$.

T a b l e 1. Initial data and obtained values of the absolute POCs π_{im} for langasite crystals

N	m	k	i	σ_{im}^0; $\sigma_{im}'^0$, kG/cm	π_{im}, Br	$\frac{\delta\Delta_k}{d_k\sigma_m}$, Br	$\frac{\delta\Delta_k(\pi_{im})}{\delta\Delta_k}$, %	$\frac{\delta\Delta_k)(S_{km})}{\delta\Delta_k}$, %
1	1	2	1;3	$\sigma_{11}^0=106$; $\sigma_{11}'^0=98.5$	$\pi_{11}=-0.14\pm0.1$	–3.15	–15	115
2	1′	2	1;3	$\sigma_{31}^0=52$; $\sigma_{31}'^0=57.5$	$\pi_{31}=+0.65\pm0.18$	–5.9	38	62
3	1	3	1;2	$\sigma_{11}^0=375$; $\sigma_{11}'^0=305$	$\pi_{11}=-0.2\pm0.04$	–1.0	–70	170
4	1′	3	1;2	$\sigma_{21}^0=185$; $\sigma_{21}'^0=140$	$\pi_{21}=+0.1\pm0.07$	–2.0	17	83
5	2	1	2;3	$\sigma_{22}^0=108$; $\sigma_{22}'^0=106$	$\pi_{22}=-0.18\pm0.1$	–3.0	–21	121
6	2′	1	2;3	$\sigma_{32}=54$; $\sigma_{32}'^0=50$	$\pi_{32}=+0.75\pm0.2$	–6.25	42	58
7	2	3	1;2	$\sigma_{12}^0=170$; $\sigma_{12}'^0=150$	$\pi_{22}=-0.16\pm0.04$	–1.1	–49	149
8	2′	3	1;2	$\sigma_{22}=300$; $\sigma_{22}'^0=275$	$\pi_{12}=+0.1\pm0.07$	–2.0	17	83
9	3	1	2;3	$\sigma_{23}^0=140$; $\sigma_{23}'^0=103$	$\pi_{23}=+0.3\pm0.08$	–2.7	38	62
10	3′	1	2;3	$\sigma_{33}^0=-135$; $\sigma_{33}'^0=-100$	$\pi_{33}=-1.3\pm0.08$	+2.8	159	–59
11	3	2	1;3	$\sigma_{13}^0=110$; $\sigma_{13}'^0=130$	$\pi_{13}=+0.3\pm0.08$	–2.7	38	62
12	3′	2	1;3	$\sigma_{33}^0=-115$; $\sigma_{33}'^0=-150$	$\pi_{33}=-1.2\pm0.07$	+2.5	167	–67
13	$\bar{4}$	4	1;$\bar{4}$	$\sigma_{\bar{4}4}^0=122$; $\sigma_{\bar{4}4}'^0=102$	$\pi_{14}=+0.32\pm0.15$	–2.5	5.5	95
14	$\bar{4}'$	4	1;$\bar{4}$	$\sigma_{\bar{4}4}^0=101$; $\sigma_{\bar{4}4}'^0=86$	$\pi_{44}=+0.35\pm0.16$	–3.4	32	68
15	4	$\bar{4}$	1;4	$\sigma_{14}^0=75.5$; $\sigma_{14}'^0=87$	$\pi_{14}=+0.32\pm0.15$	–3.6	35	65
16	4′	$\bar{4}$	1;4	$\sigma_{44}^0=170$; $\sigma_{44}'^0=220$	$\pi_{44}=+0.35\pm0.16$	–1.7	–36	136
17	1	$\bar{4}$	1;4	$\sigma_{11}^0=67.5$; $\sigma_{11}'^0=119$	$\pi_{11}=-0.16\pm0.13$	–3.8	–14	114
18	1′	$\bar{4}$	1;4	$\sigma_{\bar{4}1}^0=44$; $\sigma_{\bar{4}1}'^0=51$	$\pi_{41}=+0.3\pm0.1$	–6.65	35	65
19	1	4	1;$\bar{4}$	$\sigma_{11}^0=600$; $\sigma_{11}'^0=940$	$\pi_{11}=-0.16\pm0.02$	–0.45	–122	222
20	1′	4	1;$\bar{4}$	$\sigma_{\bar{4}1}^0=205$; $\sigma_{\bar{4}1}'^0=260$	$\pi_{41}=+0.36\pm0.14$	–1.05	4	96

4. The Results of Determination of Absolute POCs π_{im} and Their Analysis

The results of our comprehensive studies of the absolute POE are listed in Table 1. The following issues should be emphasized.

1. Langasite is related to the crystals of symmetry class 32 and is characterized by eight independent coefficients π_{im} [3, 10]. The differences between the values of principal POCs π_{im} ($i = 1, 2, 3$) that were obtained in different experimental geometries (for example, the POC $\pi_{11} = \pi_{22}$ possesses six variants), do not exceed the error typical of interferometric piezo-optical experiments ($\pm 10\%$). This evidences for the reliability of the results obtained in this work. Besides the mentioned POCs π_{11} and π_{22}, as well as π_{33}, this also concerns the symmetrically identical matrix elements $\pi_{12} = \pi_{21}$, $\pi_{13} = \pi_{23}$, and $\pi_{31} = \pi_{32}$.

As regards nonprincipal POCs, a detailed analysis of the π_{41} values obtained in different experimental geometries was carried out in Section 3. The values of π_{14}, as well as those of π_{44} – see rows 13 to 16 in Table 1 – turned out identical, because π_{14} was determined on the basis of all σ^0_{14} values (see Eq. (17)), and π_{44} on the basis of all σ^0_{44} ones (see Eq. (20)). The values of those POCs were duplicated in rows 13 to 16 only in order to use them in the calculations of piezo-optical and elastic contributions to the induced variations of the optical path length $\delta\Delta_k$ for different experimental conditions (see discussion below, in item 3).

2. Let us analyze the determination errors for π_{im} in specific experimental geometries. It bursts upon the eye that, in some experimental geometries, the determination errors for π_{im}, which are tabulated in Table 1, are comparable with the very π_{im} values. It is true, e.g., for the coefficients π_{11} (row 1), π_{21} (row 4), and π_{12} (row 8). This result can be explained as an outcome of the typical procedure of error calculation, which proceeds from the assumption that the typical error of piezo-optical experiments, $\beta = \pm 10\%$, governs the determination error for half-wave, σ_{im}, or driving, σ^0_{im}, stress values. For instance, let us calculate – by formula (8) – the coefficient π_{11} for the initial data exposed in row 1 of Table 1:

$$\pi_{11} = -\frac{\lambda}{2n_1^3 d_2}\left(\frac{1}{\sigma_{11}} + \frac{1}{\sigma'_{11}}\right) + \frac{2S_{12}}{n_1^3}(n_1 - 1) =$$

$$= -\frac{\lambda}{2n_1^3}\left(\frac{1}{\sigma^0_{11}} + \frac{1}{{\sigma'_{11}}^0}\right) + \frac{2S_{12}}{n_1^3}(n_1 - 1) =$$

$$= 0.92 \text{ Br} - 1.06 \text{ Br} = -0.14 \text{ (Br)} \qquad (24)$$

The determination error of π_{11} can be found, by assuming the relative error of $\pm 10\%$ for the sum $1/\sigma^0_{11} + 1/\sigma'^0_{11}$ (this is an objective error that has been verified by multiple measurements of the σ_{im} and σ'_{im} values) and the relative error of $\pm 5\%$ for S_{12}. Notice that the elastic coefficients were determined in work [2] by the acoustic method which provides a higher accuracy (of about 1%). However, such shortcomings of the static experiment as the non-uniformity of a mechanical stress over the specimen, the certain out-of-parallelism of crystal faces along the direction of the force F_m, the error $\delta^* d_k$ induced by crystal tapering (see Fig. 1), and others result in variations of the deformation δd_k in expression (1) and, correspondingly, the "elastic" term in formula (3) by the value of about $\pm 5\%$ (such an estimate was obtained according to the analysis of our experimental data connected with the determination of certain coefficients S_{km} for $LiNbO_3$ crystals by speckle-interferometry measurements [12, 13]). Therefore, the use of S_{km} values with a relative error of $\pm 5\%$ in the calculations of π_{im} seems justified. Taking the aforesaid into account, estimation (24) reads

$$\pi_{11} = (0.92 \pm 0.09(\text{i.e. } \pm 10\%)) -$$

$$-(1.06 \pm 0.05(\text{i.e. } \pm 5\%)) = -(0.14 \pm 0.1) \text{ Br}$$

(here, the absolute error of ± 0.1 Br – or 70% of the π_{11} amplitude – is a root-mean-square error of two terms). Such a record of the evaluation of the π_{11} amplitude demonstrates that its large relative error is caused by the fact that the amplitude itself is a result of summation of two large terms which are comparable by absolute value but have different signs. If those terms would have the same sign, the absolute and relative errors would have been considerably smaller (see, e.g., estimations for π_{33} in rows 10 and 12 of Table 1). It is evident that the determination errors for π_{im} are small if either of the terms is much larger by absolute value than the other; different signs of such terms affect the total error value to a less extent (see, e.g., π_{11} in row 19 of Table 1).

There is one more important remark. Table 1 demonstrates that the determination errors for π_{11} ($= \pi_{22}$) in various experimental geometries span from 0.02 (row 19) to 0.13 Br (row 17), or from 12.5 to 80%. However, the deviations of these POC values from the average one (-0.17 Br) do not exceed $\pm 18\%$. Such a beneficial result can be achieved only due to multiple

measurements of σ_{im} values in the given experimental geometry, including the specimen remounting, and the further averaging of the results. This requirement must be fulfilled in the case of small π_{im} values, which are formed by terms that are comparable by value. It is clear that, in the case of large π_{im}, the number of measurements can be reduced.

3. Knowing the values of the coefficients π_{im} and S_{km}, one can calculate the magnitudes of piezo-optical and elastic contributions (the augend and the addend, respectively, on the right-hand side of formula (3)) to the variation of the optical path length $\delta\Delta_k$. The specific values of those contributions to $\delta\Delta_k$, as well as the values of $\delta\Delta_k$ with respect to a unit mechanical stress σ_m and a unit specimen thickness in the direction of beam propagation (hereinafter referred to as a specific variation of the optical path length), are listed in the last three columns of Table 1. We emphasize the following.

(i) The largest total POE, i.e. the greatest value of the specific variation of the optical path length $\delta\Delta_k/(d_k\sigma_m) = (5.9 \div 6,65)$ Br, is characteristic of only 3 experimental geometries among 20 ones (see rows 2, 6, and 18). Therefore, those geometries should be most effective from the application viewpoint (if the crystal is used for the photoelastic modulation of light).

(ii) In all the cases, except for the results exposed in rows 10 and 12, the specific variation of the optical path length is negative, i.e. the application of the mechanical stress of compression, to which the minus sign is attributed, gives rise to an increase of the optical path length in the specimen. This fact perfectly correlates with experimentally determined positive signs of the σ^0_{im} values (see columns 6 and 7 in Table 1). Only in the case of the atypically large – for langasite – negative coefficient π_{33} (rows 10 and 12), the application of a compression stress is accompanied by a reduction of the optical path length.

(iii) In every case, except for the already mentioned one for π_{33}, the elastic contribution prevails over the piezo-optical one. This is associated with the fact that the elastic coefficients S_{km} for langasite are relatively large. For instance, although the POC values for langasite are somewhat smaller than those for the reference $LiNbO_3$ crystal [11], the values of the coefficients S_{km}, on the contrary, are several times larger.

In this aspect, of interest are the experimental geometries 1, 4, 8, 17, and, especially, 13 and 20, for which the magnitudes of the piezo-optical contribution to $\delta\Delta_k$ are comparable or even smaller than the determination errors for π_{im} in those experimental geometries. Hence, we may assert that the total POE (the variation of the $\delta\Delta_k$ value) is formed within the determination error limits of π_{im} owing exclusively to the elastic deformation. This means that the POE is apparent in such cases.

The explanation of this fact for cases 1, 4, 8, and 17 is simple: the coefficients π_{11} and $\pi_{12} = \pi_{21}$ are small (close to zero within the limits of their determination error). In order to substantiate the apparent POE in cases 13 and 20, formulas (9) and (10) should be used. For example, Eq. (9) demonstrates that the piezo-optical contribution to $\delta\Delta_4$ in the experimental geometry $k = 4$ and $m = \bar{4}$ is not formed by a single POC; contributing are a number of coefficients, whose common contribution $(\pi_{12} + \pi_{13} - \pi_{14})$ equals $+(0.08 \pm 0.13)$ Br, so that it is also close to zero within the limits of indicated error (the latter is determined as a root-mean-square determination error of π_{im}'s engaged). At the same time, the sum of those S_{km} coefficients, which make the elastic contribution to $\delta\Delta_4$, is large and amounts to $-(10.4 \pm 1.2)$ Br. Note that the large number of experimental geometries, where the POE is apparent, is a characteristic feature of langasite crystals.

5. Determination of the Retardation and Birefringence POCs

In order to verify the reliability of the values obtained for the absolute POCs π_{im}, we carried out a number of polarization-optical experiments and calculated the birefringence POCs π^*_{km} by the formula

$$\pi^*_{km} = -\frac{2\delta\Delta n_k}{\sigma_m}. \tag{25}$$

First, on the basis of experimental data, we determined the retardation POCs

$$\pi^0_{km} = -\frac{2\delta(\Delta n_k d_k)}{d_k\sigma_m}. \tag{26}$$

For the half-wave method of researches, $\delta(\Delta n_k d_k) = \lambda/2$, and expression (26) reads

$$\pi^0_{km} = -\lambda/(d_k\sigma_{km}) = -\lambda/\sigma^0_{km}, \tag{27}$$

where σ_{km} is the half-wave stress in the specimen, and $\sigma^0_{km} = d_k\sigma_{km}$ is the driving stress in the material across the retardation. Note that the quantities σ^0_{km} and σ_{km}, the values of which are determined from polarization-optical experiments, should be distinguished from the quantities σ^0_{im} and σ_{im}, which were introduced in Sections 2, and 3, for the interferometric study of POE.

The coefficients π^*_{km} are determined in terms of π^0_{km} as follows [9]:

$$\pi^*_{km} = \pi^0_{km} + \Delta n_k S_{km}. \tag{28}$$

On the other hand, the POCs π^*_{km} can be found from the absolute POCs π_{im}. Using Eq. (25), we have

$$\pi^*_{km} = -\frac{2}{\sigma_m}(\delta n_i - \delta n_j). \tag{29}$$

Substituting the expressions for δn_i and δn_j from the main equation of piezo-optics (2) into Eq. (29), we obtain

$$\pi^*_{km} \quad = \pi_{im} n_i^3 - \pi_{jm} n_j^3, \tag{30}$$

where the indices k, i, and j obey the 1–2–3–1 cyclic permutation rule. For example,

$$\pi^*_{12} = \pi_{22} n_2^3 - \pi_{32} n_3^3; \quad \pi^*_{21} = \pi_{31} n_2^3 - \pi_{11} n_3^3. \tag{31}$$

Note that expression (30) becomes satisfied for principal POCs π_{im}, if $(i, k, m) = (1, 2, 3)$. If any of the indices equals 4 or $\bar{4}$, the expressions of type (31) become more complicated. For instance, for π^*_{41} and $\pi^*_{4\bar{4}}$, we obtain

$$\pi^*_{41} = \pi_{11} n_1^3 - \frac{1}{2}(\pi_{12} + \pi_{31} + 2\pi_{41}) n_4^3, \tag{32}$$

$$\pi^*_{4\bar{4}} = \frac{1}{2}(\pi_{12} + \pi_{13} + \pi_{14}) n_1^3 -$$

$$-\frac{1}{4}(\pi_{11} + \pi_{13} - \pi_{14} + \pi_{31} + \pi_{33} - 2\pi_{41} + 2\pi_{44}) n_4^3. \tag{33}$$

While deriving the relations of types (32) and (33) from the general expression (29), the indices $(k, i, j) = (1, 4, \bar{4})$ should obey the 1–4–$\bar{4}$–1–4 cyclic permutation rule. In this case, the values of π^*_{km} ($(k, m) = (1, 4, \bar{4})$) calculated making use of either the π^0_{km} or π_{im} values perfectly correlate with one another by both their absolute values and signs. For example, expression (33) was obtained from the relation

$$\pi^*_{44} = -\frac{2}{\sigma_4}(\delta n_1 - \delta n_4), \tag{34}$$

where the expressions for δn_1 and δn_4, provided that σ_m acts along the direction $m = 4$, were taken from Eqs. (9) and (11), respectively. The values for σ^0_{km}, π^0_{km}, and π^*_{km} are quoted in Table 2.

Consider the results exhibited in Table 2.

1. The symmetrically identical coefficients π^0_{km} and π^*_{km}, which are determined from experimental data for σ^0_{km}, are approximately equal to each other by absolute value: $\pi^0_{12} \approx \pi^0_{21}$, $\pi^0_{13} \approx \pi^0_{23}$, $\pi^*_{12} \approx \pi^*_{21}$, and so on. The difference between them does not exceed the accuracy of polarization-optical experiments (5–7%).

2. The elastic contribution $2\Delta n_k S_{km}$ to π^0_{km} comprises $0.4 \div 2.3\%$, being several times smaller than the experimental accuracy. Therefore, the coefficients π^0_{km} and π^*_{km} coincide within the limits of experimental accuracy. Such a small value of the elastic contribution to π^0_{km} originates from a small value of birefringence. For comparison: birefringence in lithium niobate ($\Delta n = 0.085$) is seven times higher than that in langasite. The signs of the elastic contribution and the coefficients π^0_{km} were determined on the basis of a generalized rule formulated in detail in works [14, 15]. The signs of the

T a b l e 2. Path-difference, π^0_{km}, and birefringence, π^*_{km}, POCs for langasite crystals

N	σ^0_{km}, kG/cm	π^0_{km}, Br	$2\Delta n_k S_{km}$, Br (% of π^0_{km})	π^*_{km}, Br	
				Calculations using π^0_{km}	Calculations using π_{im}
1	$\sigma^0_{12} = +100$	$\pi^0_{12} = -6.5$	+0.1(1.5)%	$\pi^*_{12} = -6.4$	–6.05
2	$\sigma^0_{21} = +93$	$\pi^0_{21} = +6.9$	–0.1(1.5)%	$\pi^*_{21} = +6.8$	+6.05
3	$\sigma^0_{13} = -65$	$\pi^0_{13} = +9.9$	+0.04(0.4%)	$\pi^*_{13} = +9.9$	+10.8
4	$\sigma^0_{23} = -60$	$\pi^0_{23} = -10.8$	–0.04(0.47%)	$\pi^*_{23} = -10.8$	–10.8
5	$\sigma^0_{31} = 340$	$\pi^0_{31} = 1.9$	0	$\pi^*_{31} = 1.9$	1.85
6	$\sigma^0_{32} = 370$	$\pi^0_{32} = 1.75$	0	$\pi^*_{32} = 1.75$	1.85
7	$\sigma^0_{41} = +370$	$\pi^0_{41} = +1.75$	–0.015(0.9%)	$\pi^*_{41} = +1.75$	+1.65
8	$\sigma^0_{\bar{4}1} = +116$	$\pi^0_{\bar{4}1} = -5.55$	+0.07(1.3%)	$\pi^*_{\bar{4}1} = -5.5$	–6.2
9	$\sigma^0_{4\bar{4}} = +365$	$\pi^0_{4\bar{4}} = 1.75$	–0.04(23%)	$\pi^*_{4\bar{4}} = +1.7$	+1.9
10	$\sigma^0_{\bar{4}4} = -128$	$\pi^0_{\bar{4}4} = +5.05$	+0.04(0.8%)	$\pi^*_{\bar{4}4} = +5.1$	+3.7

N o t e. Indices k and m in columns 4 and 6 are the same as in other columns; the sign "+" or "−" of σ^0_{km} corresponds to whether the mechanical stress σ_m increases or decreases, respectively, the value of the natural path difference length Δ_k; the determination errors for σ^0_{km}, π^0_{km}, and π^*_{km} calculated using π^0_{km} amount to 5–7.

T a b l e 3. POE parameters in langasite and lithium niobate crystals (all values are given in terms of Br units)

Crystal	π_{11}	π_{12}	π_{13}	π_{31}	π_{33}	π_{14}	π_{41}	π_{44}	Summed $\lvert\pi_{im}\rvert$
$La_3Ga_5SiO_{11}$	–0.17	+0.1	+0.3	+0.7	–1.25	+0.32	+0.33	+0.35	3.5
$LiNbO_3$[11]	–0.47	+0.11	+2.0	+0.47	+1.6	+0.7	–1.9	0.21	7.5
Crystal	π^*_{12}	π^*_{13}	π^*_{31}	π^*_{41}	$\pi^*_{\bar{4}1}$	$\pi^*_{\bar{4}\bar{4}}$	$\pi^*_{\bar{4}4}$		Summed π^*_{km}
$La_3Ga_5SiO_{11}$	6.6	10.4	1.8	1.75	5.5	1.7	5.1		33
$LiNbO_3$[11]	10.6	6.8	6.9	30.3	12.5	5.8	3.3		76

POCs π^0_{31} and π^0_{32} have not been found, because $\Delta n_3 = 0$ in the corresponding experimental geometries; therefore, the elastic contribution is absent, and the equalities $\pi^*_{31} = \pi^0_{31}$ and $\pi^*_{32} = \pi^0_{32}$ are rigorous.

3. The largest POCs among those, for which $\pi^*_{km} \approx \pi^0_{km}$, are the symmetrically identical coefficients $\pi^*_{13} = -\pi^*_{23} \approx 10.4$ Br (the average value). Such an amplitude of the specified POCs is caused by the fact that, according to Eq. (30), they are formed by the absolute POCs $\pi_{13}$and π_{33}, the amplitudes of which are added. Moreover, the value of π_{33} is large *per se*. In particular, $\pi^*_{13} = \pi_{23}n_2^3 - \pi_{33}n_3^3 = 2.1$ Br $+ 8.7$ Br $= 10.8$ Br.

4. The corresponding values of POCs π^*_{km} calculated using π^0_{km} or π_{im} coincide with each other remarkably well (see rows 5 and 6 in Table 2), which evidences for a high reliability of determined values for the absolute POCs π_{im}. The only exception is the coefficient $\pi^*_{\bar{4}4}$; the relative deviations β of its values, which are tabulated in columns 5 and 6, from the average value are about $\pm 16\%$. Such a high value of β finds a simple explanation. Namely, the coefficient $\pi^*_{\bar{4}4}$ comprises a sum of many POCs π_{im} (see Eq. (33)). Substituting the error values for π_{im} coefficients (see Table 1) into Eq. (33), we obtain the root-mean-square error $\delta\pi^*_{\bar{4}4} = \pm 1.0$ Br, or $\pm 27\%$ of the $\pi^*_{\bar{4}4}$ value of 3.7 Br. Hence, the formal error of determining $\pi^*_{\bar{4}4}$ on the basis of relation (33) is almost twice as large as the real one. It is caused by the fact that, during a real experiment, the superposition of errors of such large amount of coefficients π_{im} with extreme values of only one sign is improbable. It is clear that the value of $\pi^*_{\bar{4}4}$ determined on the basis of $\pi^0_{\bar{4}4}$ is closer to a true one, because the determination error for $\pi^0_{\bar{4}4}$ is governed only by the error of the polarization-optical method and amounts to 5–7%.

6. Conclusions

The efficiency of applications of the material in acousto-optical light modulators is determined, first of all, by the photoelastic coefficients (piezo- and elasto-optical ones). Let us compare the POE in langasite and lithium niobate, the latter being widely used in acousto-optical devices. Table 3 displays the average values of independent POCs π_{im} and the average absolute values of POCs π^*_{km} calculated for the π_{im} and π^*_{km} data presented in Tables 1 and 2. The coefficients π_{im} for $LiNbO_3$ were taken from work [11], and the POCs π^*_{km} were calculated on the basis of the formulas of types (30)–(33) and the values of absolute POCs π_{im}.

While comparing the tabulated data, we see that, on the average, the POCs π_{im} and π^*_{km} for $LiNbO_3$ crystals are somewhat larger than the corresponding quantities for langasite. One of the comparison criteria for the POE is the sum of all POC values. By this criterion, lithium niobate is better than langasite (by a factor of 2) with respect to both the POCs π_{im} and π^*_{km}. However, some POCs for langasite are large (these are π_{33} and π^*_{13}). This means that, in a certain direction of the spatial POE surface (about such surfaces see, e.g., works [16, 17]), the magnitude of the POE in langasite crystals would be comparable with that in the extremal directions of the spatial POE surface in $LiNbO_3$ crystals. As a rule, in this case, the elasto-optical surface constructed on the basis of the matrix of elasto-optical coefficients p_{im} also has a direction which is characterized by a large effect [18]; and this is an indication that the acousto-optical efficiency of langasite and lithium niobate crystals might be comparable in some geometries of acousto-optical interaction. In such a case, langasite would have an important advantage, because it is substantially better than lithium niobate by the thermal stability of its physical characteristics.

The work has been supported by Science and Technology Center in Ukraine (Project # 3222).

1. I.A. Andreev, Zh. Tekhn. Fiz. **74**, 1 (2004).
2. A.A. Kaminskii, I.M. Silvestrova, S.E. Sarkisov et al., Phys. Status Solidi A **80**, 607 (1983).
3. *Acoustic Crystals. A Handbook*, edited by M.P. Shaskolskaya (Nauka, Moscow, 1982) (in Russian).
4. A.A. Kaminskii, B.V. Mill, G.G. Khodzhabagyan et al., Phys. Status Solidi A **80**, 387 (1983).
5. J. Stade, L. Bohaty, M. Hengst et al., Cryst. Res. Technol. **37**, 1113 (2002).

6. J. Bohm, Cryst. Growth **216**, 293 (2000).

7. I.S. Rez, Usp. Fiz. Nauk **93**, 633 (1968).

8. H. Landolt and R.L. Börnstein, *Numerical Data and Functional Relations in Science and Technology. New Series* (Springer, Berlin, 1979).

9. B. Mytsyk, Ukr. J. Phys. Opt. **4**, 1 (2003).

10. T.S. Narasimhamurty, *Photoelastic and Electro-Optic Properties of Crystals* (Plenum Press, New York, 1981).

11. B.H. Mytsyk and A.S. Andrushchak, Kristallogr. **35**, 1574 (1990).

12. R. Jones and C. Wykes, *Holographic and Speckle Interferometry* (Cambridge University Press, Cambridge, 1989).

13. V.I. Smolyak, A.L. Tkhoruk, T.I. Voronyak et al., Opt. Zh. **71**, 58 (2004).

14. B.H. Mytsyk, B.M. Karnaukh, V.V. Ostapyuk et al., *Optics of Anisotropic Media* (Moscow Physico-Technical Inst. Publ. House, Moscow, 1987) (in Russian).

15. B.H. Mytsyk, Ya.V. Pryriz, and A.S. Andrushchak, Cryst. Res. Technol. **26**, 931 (1991).

16. P. Han, W. Yan, J. Tian et al., Appl. Phys. Lett. **86**, 1 (2005).

17. B.H. Mytsyk and N.M. Dem'yanishin, Kristallogr. **51**, 693 (2006).

18. A.S. Andrushchak, Ya.V. Bobitski, M.V. Kaidan et al., Opt. Mater. **27**, 619 (2004).

Received 18.12.06.
Translated from Ukrainian by O.I. Voitenko

ПОВНЕ ВИВЧЕННЯ П'ЄЗООПТИЧНОГО ЕФЕКТУ В КРИСТАЛАХ ЛАНГАСИТУ

Б.Г. Мицик, А.С. Андрущак, Г.І. Гаськевич

Р е з ю м е

Описано особливості методики визначення абсолютних п'єзооптичних коефіцієнтів (ПОК) на реальних зразках, які мають, як правило, незначну непаралельність граней – $(2 \div 4) \cdot 10^{-2}$ град. Методику застосовано до кристалів лангаситу $La_3Ga_5SiO_{11}$. Крім абсолютних значень ПОК, які зв'язують зміни показників заломлення з механічним напруженням, визначено також ПОК двопроменезаломлення і ПОК різниці ходу. Проведено всебічну кореляцію вказаних ПОК, яка підтверджує однозначність і достовірність повного вивчення п'єзооптичного ефекту. Проведено також порівняння п'єзооптичних ефектів у кристалах лангаситу і модельних кристаталах ніобату літію. Із сумірності величин деяких ПОК обох кристалів зроблено висновок про перспективність застосування лангаситу в акустооптичних пристроях, тим більше, що ці кристали відзначаються високою температурною стабільністю фізичних характеристик.